

## Experimental Section

The FAB mass spectra were taken on a Kratos MS 50 mass spectrometer equipped with a magnet having a mass range of 10000 Da at full (8-kV) accelerating voltage. The atom beam was provided with an Ion Tech FAB gun operating with xenon at 8 kV with a current of 30-40

$\mu\text{A}$ . The magnet was typically scanned a rate of 100 s/decade.

**Acknowledgment.** We thank the SERC (UK) and Churchill College, Cambridge, for financial support.

**Registry No.** 1, 9007-92-5; 2, 9007-43-6.

## Stereochemically Constrained Peptides. Theoretical and Experimental Studies on the Conformations of Peptides Containing 1-Aminocyclohexanecarboxylic Acid

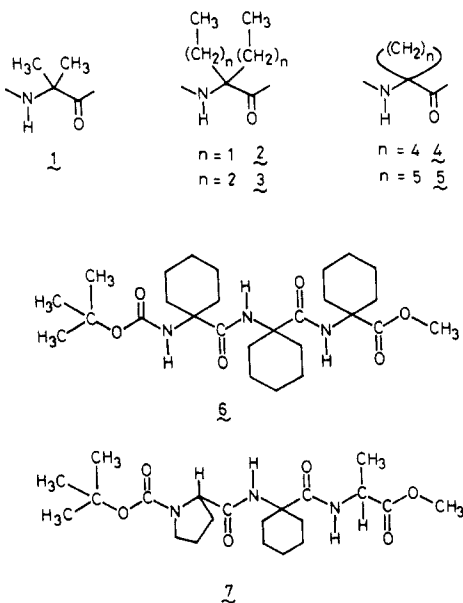
P. K. C. Paul,<sup>†</sup> M. Sukumar,<sup>†</sup> R. Bardi,<sup>‡</sup> A. M. Piazzesi,<sup>‡</sup> G. Valle,<sup>‡</sup> C. Toniolo,<sup>‡</sup> and P. Balaram\*<sup>†</sup>

Contribution from the Molecular Biophysics Unit, Indian Institute of Science, Bangalore 560 012, India, and Biopolymer Research Centre, CNR, Department of Organic Chemistry, University of Padova, 35131, Padova, Italy. Received March 27, 1986

**Abstract:** Conformational energy calculations on the model system *N*-acetyl-1-aminocyclohexanecarboxylic acid *N'*-methylamide (Ac-Acc<sup>6</sup>-NHMe), using an average geometry derived from 13 crystallographic observations, establish that the Acc<sup>6</sup> residue is constrained to adopt conformations in the  $3_{10}/\alpha$ -helical regions of  $\phi, \psi$  space ( $\phi = \pm 50 \pm 20^\circ$ ,  $\psi = \pm 50 \pm 20^\circ$ ). In contrast, the  $\alpha, \alpha$ -dialkylated residue with linear hydrocarbon side chains,  $\alpha, \alpha$ -di-*n*-propylglycine favors fully extended backbone structures ( $\phi \approx \psi \approx 180^\circ$ ). The crystal structures of two model peptides, Boc-(Acc<sup>6</sup>)<sub>3</sub>-OMe (type III  $\beta$ -turn at -Acc<sup>6</sup>(1)-Acc<sup>6</sup>(2)-) and Boc-Pro-Acc<sup>6</sup>-Ala-OMe (type II  $\beta$ -turn at -Pro-Acc<sup>6</sup>-), establish that Acc<sup>6</sup> residues can occupy either position of type III  $\beta$ -turns and the  $i + 2$  position of type II  $\beta$ -turns. The stereochemical rigidity of these peptides is demonstrated in solution by NMR studies, which establish the presence of one intramolecular hydrogen bond in each peptide in CDCl<sub>3</sub> and (CD<sub>3</sub>)<sub>2</sub>SO. Nuclear Overhauser effects permit characterization of the  $\beta$ -turn conformations in solution and establish their similarity to the solid-state structures. The implications for the use of Acc<sup>6</sup> residues in conformational design are considered.

The introduction of  $\alpha, \alpha$ -dialkylated amino acids into peptide chains provides a means of restricting the available range of backbone conformations.<sup>1</sup> The best studied member of this class of amino acids is  $\alpha$ -aminoisobutyric acid (Aib).<sup>2</sup> The Aib residue (1) has been shown to strongly stabilize conformations in the  $3_{10}/\alpha$ -helical regions of the conformational map ( $\phi \sim \pm 60 \pm 20^\circ$ ,  $\psi \sim \pm 30 \pm 20^\circ$ ).<sup>3</sup> Peptides containing the residues  $\alpha, \alpha$ -diethylglycine (Deg; 2) and  $\alpha, \alpha$ -di-*n*-propylglycine (Dpg; 3) have been shown to occur in fully extended conformations ( $\phi \sim 180^\circ$ ,  $\psi \sim 180^\circ$ ).<sup>4</sup> Preliminary studies on fully protected peptides containing 1-aminocycloalkancarboxylic acids (Acc<sup>*n*</sup>, where *n* is the number of carbon atoms in the cycloalkane ring) suggest that both 1-aminocyclopentanecarboxylic acid (Acc<sup>5</sup>, 4)<sup>5</sup> and

1-aminocyclohexanecarboxylic acid (Acc<sup>6</sup>, 5) residues<sup>6</sup> stabilize folded conformations similar to those observed in Aib peptides. A synthetic chemotactic peptide analogue formyl-Met-Acc<sup>6</sup>-Phe-OMe has been shown to possess significantly higher biological activity than the parent peptide, formyl-Met-Leu-Phe-OMe<sup>7</sup>, stimulating interest in the conformational characteristics of Acc<sup>6</sup> residues. In this report we present conformational energy calculations on Ac-Acc<sup>6</sup>-NHMe and compare the results obtained with similar computations for Aib<sup>1a,8</sup> and Dpg<sup>4a,c</sup> residues. An



(1) (a) Marshall, G. R.; Bosshard, H. E. *Circ. Res., Suppl.* **1972**, 30 and 31, 143-150. (b) Marshall, G. R.; Bosshard, H. E.; Kendrick, N. C. E.; Turk, J.; Balasubramanian, T. M.; Cobb, S. M. H.; Moore, M.; Leduc, L.; Needleman, P. In *Peptides: Proceedings of the Fourteenth European Peptide Symposium*; Loffet, A., Ed.; Editions de l'Université de Bruxelles: Brussels, Belgium, 1972; pp 361-369.

(2) (a) Abbreviations used: Aib,  $\alpha$ -aminoisobutyric acid; Acc<sup>*n*</sup>, 1-aminocycloalkancarboxylic acid with *n* atoms in the cycloalkane ring; Deg,  $\alpha, \alpha$ -diethylglycine; Dpg,  $\alpha, \alpha$ -di-*n*-propylglycine; Boc, *tert*-butoxycarbonyl; Z, benzyloxycarbonyl; pBrBz, *p*-bromobenzoyl; mClAc, monochloroacetyl; (b) All chiral amino acids used are of the L configuration. (c) Backbone torsion angles are defined according to the IUPAC-IUB Commission on Biochemical Nomenclature: *Biochemistry* **1970**, 9, 3471-3479.

(3) For leading references see: (a) Prasad, B. V. V.; Balaram, P. *CRC Crit. Revs. Biochem.* **1984**, 16, 307-348. (b) Toniolo, C.; Bonora, G. M.; Bavoso, A.; Benedetti, E.; Di Blasio, B.; Pavone, V.; Pedone, C. *Biopolymers* **1983**, 22, 205-215. (c) Bosch, R.; Jung, G.; Schmitt, H.; Winter, W. *Biopolymers* **1985**, 24, 979-999. (d) Smith, G. D.; Pletnev, V. Z.; Duax, W. L.; Balasubramanian, T. M.; Bosshard, H. E.; Czerwinski, E. W.; Kendrick, N. C. E.; Mathews, F. S.; Marshall, G. R. *J. Am. Chem. Soc.* **1981**, 103, 1493-1501.

(4) (a) Benedetti, E.; Toniolo, C.; Hardy, P.; Barone, V.; Bavoso, A.; Di Blasio, B.; Grimaldi, P.; Lelj, F.; Pavone, V.; Pedone, C.; Bonora, G. M.; Lingham, I. *J. Am. Chem. Soc.* **1984**, 106, 8146-8152. (b) Bonora, G. M.; Toniolo, C.; Di Blasio, B.; Pavone, V.; Pedone, C.; Benedetti, E.; Lingham, I.; Hardy, P. *M. J. Am. Chem. Soc.* **1984**, 106, 8152-8156. (c) Barone, V.; Bavoso, A.; Di Blasio, B.; Grimaldi, P.; Lelj, F.; Pavone, V.; Pedone, C. *Biopolymers* **1985**, 24, 1759-1767.

(5) Bardi, R.; Piazzesi, A. M.; Toniolo, C.; Sukumar, M.; Balaram, P. *Biopolymers*, in press.

(6) Bardi, R.; Piazzesi, A. M.; Toniolo, C.; Sukumar, M.; Raj, P. A.; Balaram, P. *Int. J. Pept. Protein Res.* **1985**, 25, 628-639.

(7) Sukumar, M.; Raj, P. A.; Balaram, P.; Becker, E. L. *Biochem. Biophys. Res. Commun.* **1985**, 128, 339-344.

<sup>†</sup> Indian Institute of Science.

<sup>‡</sup> University of Padova.



**Table II.** Fractional Coordinates ( $\times 10^4$ ) and Equivalent Isotropic Temperature Factors ( $\text{\AA}^2, \times 10^3$ ) for Boc-( $-\text{Acc}^6$ -) $_3$ -OMe (**6**)<sup>a</sup>

atom	x	y	z	$U_{eq}$
O(1)	3218 (2)	1367 (2)	11697 (3)	73 (2)
O(2)	2368 (2)	1167 (2)	9756 (3)	81 (2)
O(3)	2339 (2)	2111 (2)	6703 (3)	75 (2)
O(4)	-166 (2)	2480 (2)	6910 (3)	71 (2)
O(5)	-1587 (2)	1276 (2)	7026 (4)	120 (3)
O(6)	-987 (2)	1694 (2)	8958 (4)	94 (3)
N(1)	3514 (2)	1933 (2)	9931 (3)	58 (2)
N(2)	2068 (2)	2606 (2)	8602 (4)	56 (2)
N(3)	648 (2)	1680 (2)	8103 (3)	50 (2)
C(1)	1774 (5)	1080 (6)	12370 (9)	139 (7)
C(2)	3224 (7)	957 (6)	13821 (6)	139 (7)
C(3)	2848 (8)	156 (4)	11909 (9)	140 (7)
C(4)	2744 (4)	871 (3)	12425 (5)	84 (3)
C(5)	2999 (3)	1470 (3)	10408 (5)	61 (3)
C(6)	3516 (3)	2026 (3)	8525 (4)	60 (3)
C(7)	4142 (3)	2634 (3)	8316 (5)	84 (3)
C(8)	5130 (4)	2456 (5)	8705 (5)	119 (5)
C(9)	5384 (5)	1801 (6)	8038 (9)	162 (7)
C(10)	4793 (5)	1205 (5)	8335 (8)	132 (6)
C(11)	3809 (3)	1374 (4)	7868 (6)	89 (4)
C(12)	2571 (3)	2244 (3)	7859 (5)	57 (3)
C(13)	1181 (3)	2889 (2)	8133 (4)	58 (3)
C(14)	1224 (4)	3423 (3)	7035 (6)	81 (4)
C(15)	1735 (5)	4057 (4)	7494 (8)	123 (5)
C(16)	1320 (7)	4400 (4)	8613 (9)	141 (7)
C(17)	1310 (5)	3898 (4)	9744 (8)	116 (5)
C(18)	821 (4)	3240 (3)	9297 (5)	80 (4)
C(19)	521 (3)	2323 (2)	7649 (4)	52 (3)
C(20)	-1 (3)	1137 (2)	7674 (4)	53 (3)
C(21)	49 (3)	943 (3)	6237 (5)	71 (3)
C(22)	903 (4)	564 (3)	6067 (6)	93 (4)
C(23)	974 (4)	-96 (3)	6871 (7)	109 (5)
C(24)	967 (4)	79 (3)	8303 (7)	100 (4)
C(25)	172 (4)	500 (3)	8532 (5)	79 (4)
C(26)	-940 (3)	1386 (3)	7810 (6)	76 (3)
C(27)	-1860 (5)	1928 (7)	9185 (14)	151 (8)

<sup>a</sup> esd's are given in parentheses.

of 293 K, with a peptide concentration of 0.05 M. Undegassed samples were used in the NOE experiments. Difference NOE spectra<sup>14</sup> were obtained by sequential recording of perturbed and normal spectra (8K memory each) with low-power on-resonance saturation of a peak and by off-resonance shifting of the irradiation frequency, respectively. A delay time of 3.0 s was used between transients. The difference free induction decay was multiplied by a decaying exponential, prior to Fourier transformation.

## Results and Discussion

**Average Geometry and Theoretical Calculations.** The average geometry derived for the  $\text{Acc}^6$  residue from an analysis of available crystal structures is summarized in Figure 1. The bond angles at the  $\text{C}^\alpha$  atom of the  $\text{Acc}^6$  residue show deviations from tetrahedral values, which are similar to those observed for the Aib residue.<sup>8c</sup> An asymmetric geometry similar to Aib is obtained. The mean endocyclic torsion angle of  $\pm 54.6^\circ$  is consistent with an almost perfect chair conformation, for the cyclohexane side chain in the  $\text{Acc}^6$  residue.<sup>15</sup> In almost all crystal structures containing  $\text{Acc}^6$ , described so far,<sup>6,9</sup> the amino group occupies the axial position, in accordance with early expectations.<sup>16</sup> The only exception is the crystal structure of the free amino acid (H- $\text{Acc}^6$ -OH), where the carboxyl group occupies an axial position.<sup>9a</sup> Interestingly, the amino group occupies the axial position in the structure of the amino acid hydrochloride (H- $\text{Acc}^6$ -OH-HCl).<sup>17</sup>

Conformational energy maps have been computed for Ac- $\text{Acc}^6$ -NHMe with both axial and equatorial orientations of the

**Table III.** Fractional Coordinates ( $\times 10^4$ ), Population Parameters (pp), and Equivalent Isotropic Temperature Factors ( $\text{\AA}^2, \times 10^3$ ) for Boc-L-Pro- $\text{Acc}^6$ -L-Ala-OMe (**7**)<sup>a</sup>

atom	pp	x	y	z	$U_{eq}/U^*$
O(1)	1.0	3894	8620	316	79 (3)
O(2)	1.0	1825 (5)	7960 (6)	130 (9)	65 (3)
O(3)	1.0	2052 (6)	4990 (7)	1877 (8)	73 (3)
O(4)	1.0	-916 (6)	5236 (6)	4391 (8)	61 (3)
O(5)	1.0	-2618 (6)	7716 (8)	3463 (9)	84 (4)
O(6)	1.0	-1603 (5)	8076 (6)	7222 (8)	62 (3)
N(1)	1.0	3158 (6)	6460 (7)	-1020 (12)	63 (3)
N(2)	1.0	180 (5)	4833 (6)	-895 (9)	41 (3)
N(3)	1.0	-260 (6)	6829 (6)	2579 (10)	55 (3)
C(1)	1.0	2857 (12)	10789 (12)	530 (23)	103 (9)
C(2)	1.0	5231 (11)	10607 (13)	1599 (23)	103 (8)
C(3)	1.0	3881 (14)	9887 (17)	4104 (18)	128 (9)
C(4)	1.0	3927 (9)	10019 (9)	1655 (15)	71 (5)
C(5)	1.0	2866 (7)	7702 (8)	-156 (11)	51 (4)
C(6)	1.0	2160 (7)	5334 (8)	-1964 (12)	51 (4)
C(7)	1.0	2896 (9)	4102 (9)	-2665 (16)	73 (5)
C(8)	0.6	4225 (20)	4385 (21)	-1133 (34)	104 (5)*
C(80)	0.4	4075 (20)	4829 (23)	-3368 (38)	74 (6)*
C(9)	1.0	4415 (10)	6059 (13)	-1275 (28)	135 (9)
C(10)	1.0	1469 (7)	5035 (7)	-75 (12)	50 (4)
C(11)	1.0	-676 (7)	4422 (7)	512 (11)	44 (3)
C(12)	1.0	-371 (8)	3022 (8)	1218 (12)	64 (4)
C(13)	1.0	-640 (9)	1860 (8)	-876 (14)	64 (4)
C(14)	1.0	-2028 (9)	1778 (9)	-2241 (15)	72 (5)
C(15)	1.0	-2386 (8)	3150 (8)	-2966 (13)	60 (4)
C(16)	1.0	-2050 (7)	4338 (7)	-923 (12)	50 (4)
C(17)	1.0	-563 (7)	5532 (8)	2680 (11)	46 (4)
C(18)	1.0	-307 (8)	7919 (8)	4527 (12)	51 (4)
C(19)	1.0	4 (11)	9316 (9)	3938 (18)	89 (7)
C(20)	1.0	-1671 (7)	7863 (7)	4892 (11)	51 (4)
C(21)	1.0	-2863 (9)	8077 (11)	7715 (16)	76 (6)

<sup>a</sup> esd's are given in parentheses.

amino group. The results are shown in Figure 2. Energy maps for Ac-Aib-NHMe and Ac-Dpg-NHMe using identical procedures are shown for comparison in Figure 3. Several noteworthy features emerge from these results.

In the  $\text{Acc}^6$  (-NH- axial) case the deepest energy minima lie in the right- and left-handed  $\alpha/3_{10}$ -helical region (region I) of  $\phi, \psi$  space. A minimum is also observed for a quasiextended conformation (region II,  $\phi = \pm 60^\circ, \psi \sim 180^\circ$ ). There is also a limited region (region III) of energetically accessible conformations corresponding to  $\text{C}_7$  structures ( $3 > 1$  hydrogen bonded). For the  $\text{Acc}^6$  (-NH- equatorial) case region II shoots up in energy ( $\sim 25 \text{ kcal mol}^{-1}$  above the minimum), while a new quasiextended structure is stabilized (region II',  $\phi \sim 180^\circ, \psi \sim \pm 60^\circ$ ). It is clear that 1,3-diaxial interactions between the axial substituent and the axial  $\text{C}^\gamma\text{H}$  groups determine the preference for the quasiextended region. Regions with  $\phi \sim 180^\circ$  are strongly disallowed when the -NH- group is axial, while the  $\psi \sim 180^\circ$  regions are extremely high in energy for the -CO- axial case. The lowest energy conformations occur at the grid points  $\phi = \pm 52^\circ, \psi = \pm 46^\circ$  (-NH- axial) and  $\phi = \pm 48^\circ, \psi \sim \pm 60^\circ$  (-NH- equatorial). The -NH- axial minimum is  $\sim 1.6 \text{ kcal mol}^{-1}$  lower in energy than the -NH- equatorial minimum. Perspective views of the low-energy conformations of Ac- $\text{Acc}^6$ -NHMe are shown in Figure 4.

In the case of Ac-Aib-NHMe (Figure 3a) energetically accessible conformations are observed in the  $\alpha$ -helical ( $\phi \sim \pm 55^\circ, \psi \sim \pm 45^\circ$ ),  $\text{C}_7$  ( $\phi \sim \pm 70^\circ, \psi \sim \mp 70^\circ$ ), fully extended ( $\phi \sim 180^\circ, \psi \sim 180^\circ$ ), and quasiextended ( $\phi \sim 180^\circ, \psi \sim \pm 60^\circ$  or  $\phi \sim \pm 60^\circ, \psi \sim 180^\circ$ ) regions. The lowest energy conformation is observed at  $\phi \sim \pm 50^\circ, \psi \sim \pm 48^\circ$ . These observations are in complete agreement with earlier reports.<sup>8</sup>

The conformational energy map for Ac-Dpg-NHMe (Figure 3b) shows energy minima in the helical, fully extended, and quasiextended regions. The lowest energy conformation occurs in the fully extended region ( $\phi \sim 180^\circ, \psi \sim 180^\circ$ ) and is about  $3 \text{ kcal mol}^{-1}$  lower than the minimum in the helical region. In Ac-Dpg-NHMe, 81 side chain conformations are possible for each

(14) Rao, B. N. N.; Kumar, A.; Balaram, H.; Ravi, A.; Balaram, P. *J. Am. Chem. Soc.* **1983**, *105*, 7423-7428.

(15) Bixon, M.; Lifson, S. *Tetrahedron* **1967**, *23*, 769-784.

(16) Kenner, G. W.; Preston, J.; Sheppard, R. C. *J. Chem. Soc.* **1965**, 6239-6244.

(17) Chacko, K. K.; Srinivasan, R.; Zand, R. *J. Cryst. Mol. Struct.* **1971**, *1*, 261-269.

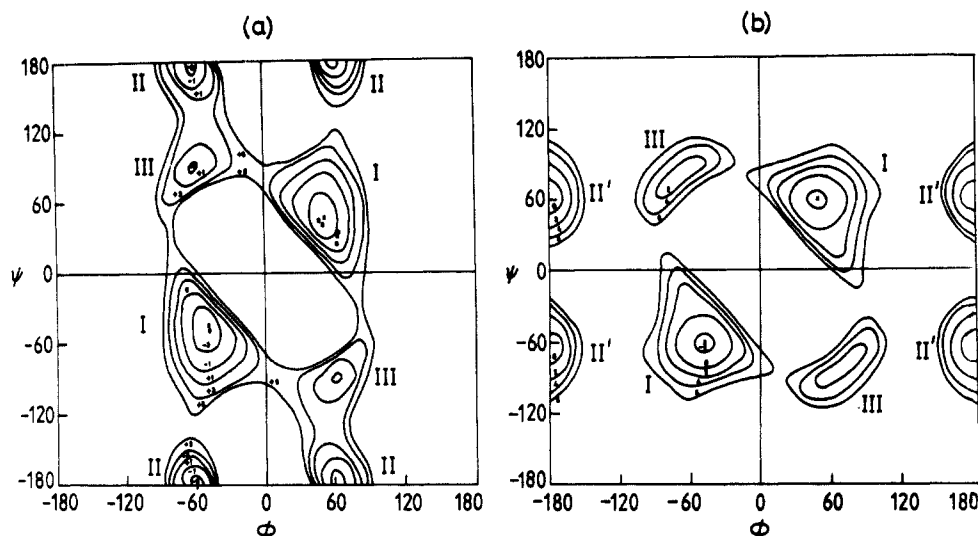


**Figure 2.** Conformational energy maps for Ac-Acc<sup>6</sup>-NHMe: (a) -NH- axial, (b) -NH- equatorial. The lowest energy conformations are indicated (X) and the energy contours are drawn in steps of 2 kcal mol<sup>-1</sup>. The crystallographically observed  $\phi$ ,  $\psi$  values (●) in Boc-Met-Acc<sup>6</sup>-OMe, Boc-Aib-Acc<sup>6</sup>-OMe, Boc-Aib-Acc<sup>6</sup>-NHMe, Boc-(Acc<sup>6</sup>)<sub>3</sub>-OMe, and Boc-Pro-Acc<sup>6</sup>-Ala-OMe are indicated.

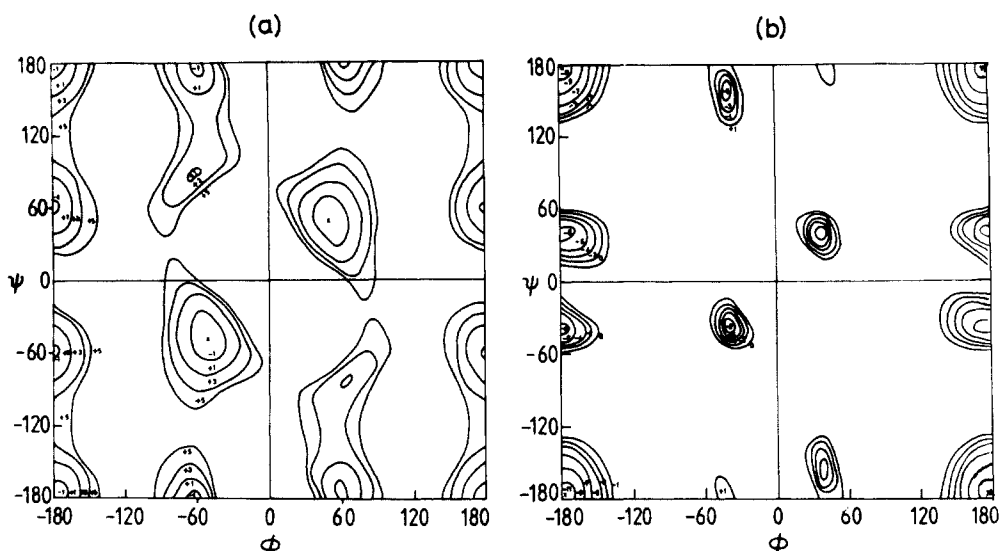


**Figure 3.** Conformational energy maps for (a) Ac-Aib-NHMe and (b) Ac-Dpg-NHMe. The map shown corresponds to side chain conformations  $\chi_1$ ,  $\chi_2$  of 60°, 180° and -60°, 180° for the L and D side chains, respectively.

$\phi$ ,  $\psi$  value considering the gauche<sup>+</sup> ( $g^+$ ), gauche<sup>-</sup> ( $g^-$ ), and trans ( $t$ ) rotamers about the C <sup>$\alpha$</sup> -C <sup>$\beta$</sup>  and C <sup>$\beta$</sup> -C <sup>$\gamma$</sup>  bonds of both  $n$ -propyl groups. Of these only the 9 symmetric cases were considered. The results establish that the  $g^-g^-$ ,  $g^-t$ ,  $g^-g^+$ ,  $tg^-$ ,  $tt$ , and  $tg^+$  (for the *pro-S* substituent) are energetically very unfavorable due to side chain-side chain short contacts. Further the  $g^+g^+$  (*pro-S*) conformation is completely disallowed by side chain-backbone contacts in the entire  $\phi$ - $\psi$  plane. Of the remaining two,  $g^+t$  (*pro-S*) has better energies at all regions of  $\phi$ ,  $\psi$  space as compared to  $g^+g^-$  (*pro-S*), and this energy map is shown in Figure 3b. The results are in general agreement with those obtained by an energy minimization procedure, with the exception that the  $g^+g^-$  conformations were favored in the fully extended regions, in the earlier study.<sup>4a</sup> It may be noted that only  $g^+t$  ( $g^-t$ ) conformations have indeed been observed in the crystal structures of Dpg peptides, so far.<sup>4a</sup> A comparison of the maps in Figures 2 and 3 suggests that the Acc<sup>6</sup> residue is largely compelled to adopt conformations in the  $\alpha$ -helical region with fully extended structures being completely ruled out. In contrast such conformations are indeed *highly likely* for Dpg residues, an expectation<sup>4a,c</sup> which has received some experimental support.<sup>4b</sup> For Aib, conformations in the  $3_{10}/\alpha$ -helical regions are favored, as already been borne out in extensive investigations.<sup>3</sup> However, the occasional observation of Aib in extended (quasi or fully) and C<sub>7</sub> regions in crystal structures<sup>3a</sup>

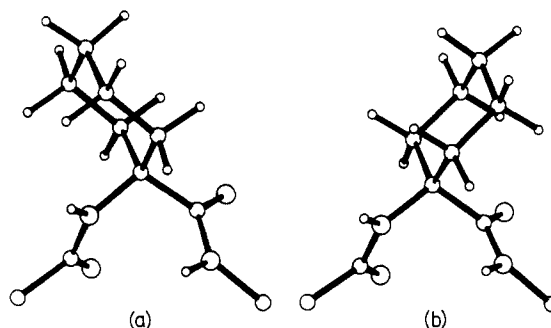


**Figure 4.** Perspective drawings of low-energy conformations of Ac-Acc<sup>6</sup>-NHMe: (a) -NH- axial  $\phi = -52^\circ$ ,  $\psi = -46^\circ$ , (b) -NH-equatorial  $\phi = -48^\circ$ ,  $\psi = -60^\circ$ .

is in agreement with conformational energy calculations.

In order to provide experimental support for the conformational energy calculations summarized above, we describe structural studies on two Acc<sup>6</sup> containing protected tripeptides, Boc-(Acc<sup>6</sup>)<sub>3</sub>-OMe (6) and Boc-Pro-Acc<sup>6</sup>-Ala-OMe (7).

**Crystal Structures of Peptides 6 and 7.** The molecular conformations of peptides 6 and 7, determined in the solid state by X-ray diffraction, are shown in Figures 5 and 6, while the mo-

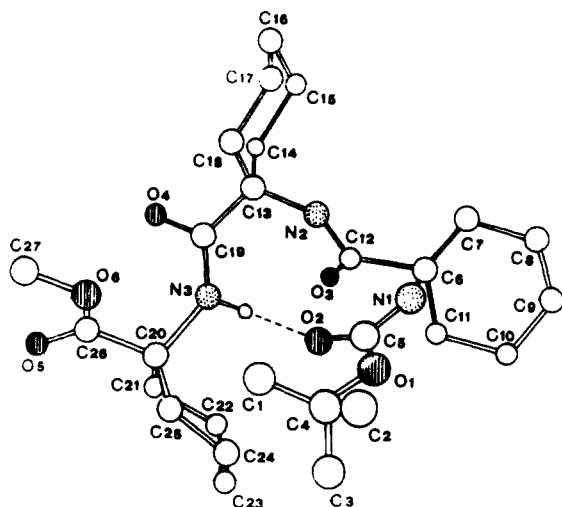
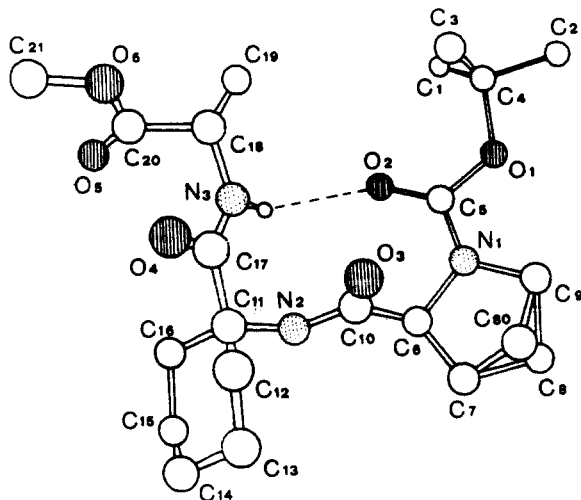
Table IV. Backbone Torsional Angles (deg)<sup>a</sup> in Peptides 6 and 7

Boc-(Acc <sup>6</sup> ) <sub>3</sub> -OMe (6)			Boc-Pro-Acc <sup>6</sup> -Ala-OMe (7)		
$\omega_{\text{Acc}^6(1)}$	O(1)-C(5)-N(1)-C(6)	-167.5 (4)	$\omega_{\text{Pro}}$	O(1)-C(5)-N(1)-C(6)	-171.5 (7)
$\phi_{\text{Acc}^6(1)}$	C(5)-N(1)-C(6)-C(12)	60.8 (6)	$\phi_{\text{Pro}}$	C(5)-N(1)-C(6)-C(10)	-60.1 (9)
$\psi_{\text{Acc}^6(1)}$	N(1)-C(6)-C(12)-N(2)	29.5 (6)	$\psi_{\text{Pro}}$	N(1)-C(6)-C(10)-N(2)	136.6 (7)
$\omega_{\text{Acc}^6(2)}$	C(6)-C(12)-N(2)-C(13)	176.6 (4)	$\omega_{\text{Acc}^6}$	C(6)-C(10)-N(2)-C(11)	174.9 (6)
$\phi_{\text{Acc}^6(2)}$	C(12)-N(2)-C(13)-C(19)	60.5 (6)	$\phi_{\text{Acc}^6}$	C(10)-N(2)-C(11)-C(17)	61.5 (9)
$\psi_{\text{Acc}^6(2)}$	N(2)-C(13)-C(19)-N(3)	24.9 (6)	$\psi_{\text{Acc}^6}$	N(2)-C(11)-C(17)-N(3)	29.1 (9)
$\omega_{\text{Acc}^6(3)}$	C(13)-C(19)-N(3)-C(20)	178.0 (4)	$\omega_{\text{Ala}}$	C(11)-C(17)-N(3)-C(18)	172.3 (7)
$\phi_{\text{Acc}^6(3)}$	C(19)-N(3)-C(20)-C(26)	-49.6 (5)	$\phi_{\text{Ala}}$	C(17)-N(3)-C(18)-C(20)	-58.2 (9)
$\psi_{\text{Acc}^6(3)}$	N(3)-C(20)-C(26)-O(6)	-45.8 (6)	$\psi_{\text{Ala}}$	N(3)-C(18)-C(20)-O(6)	139.3 (6)

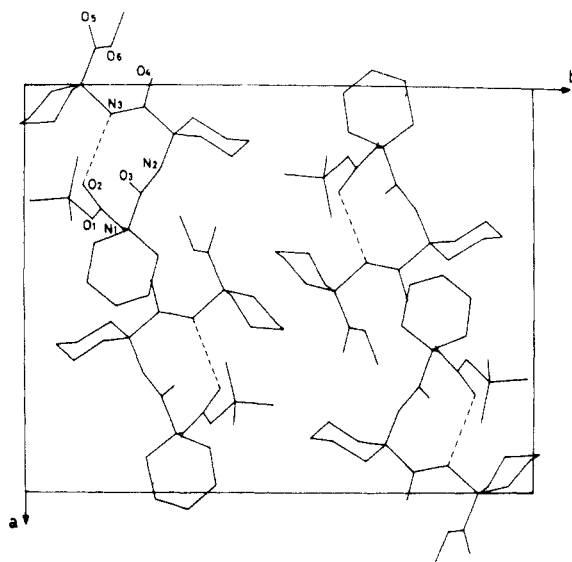
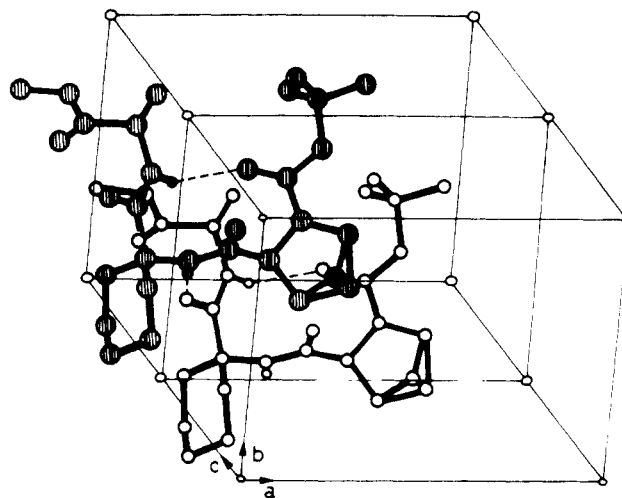
<sup>a</sup>esd's are given in parentheses. Torsion angles are given for one enantiomeric molecule.

Table V. Geometry of Hydrogen Bonds in the Crystals of 6 and 7

donor D-H	acceptor A	symmetry equivalence of A	distances (Å)		angle (deg) D-H...A
			D...A	H...A	
Boc-(Acc <sup>6</sup> ) <sub>3</sub> -OMe (6)					
N(3)-H	O(2)	<i>x,y,z</i>	3.076 (5)	2.091 (5)	167.8 (4)
N(1)-H	O(4)	$\frac{1}{2} + x, \frac{1}{2} - y, \frac{1}{2} + z$	2.890 (5)	1.924 (5)	161.1 (4)
Boc-Pro-Acc <sup>6</sup> -Ala-OMe (7)					
N(3)-H	O(2)	<i>x,y,z</i>	3.21 (1)	2.38 (1)	140.1 (6)
N(2)-H	O(4)	<i>x,y,z</i> - 1	2.90 (1)	1.90 (1)	179.5 (7)

Figure 5. Molecular conformation of Boc-(Acc<sup>6</sup>)<sub>3</sub>-OMe (6) in the solid state.Figure 6. Molecular conformation of Boc-Pro-Acc<sup>6</sup>-Ala-OMe (7) in the solid state. Note that C<sup>γ</sup> Pro occupies two distinct positions.

lecular packing in the crystals is illustrated in Figures 7 and 8, respectively. The relevant backbone torsion angles<sup>2</sup> are listed in

Figure 7. Molecular packing in crystals of Boc-(Acc<sup>6</sup>)<sub>3</sub>-OMe (6) viewed down the *c* axis.Figure 8. Molecular packing in crystals of Boc-Pro-Acc<sup>6</sup>-Ala-OMe (7). Note that there is only one molecule per unit cell.

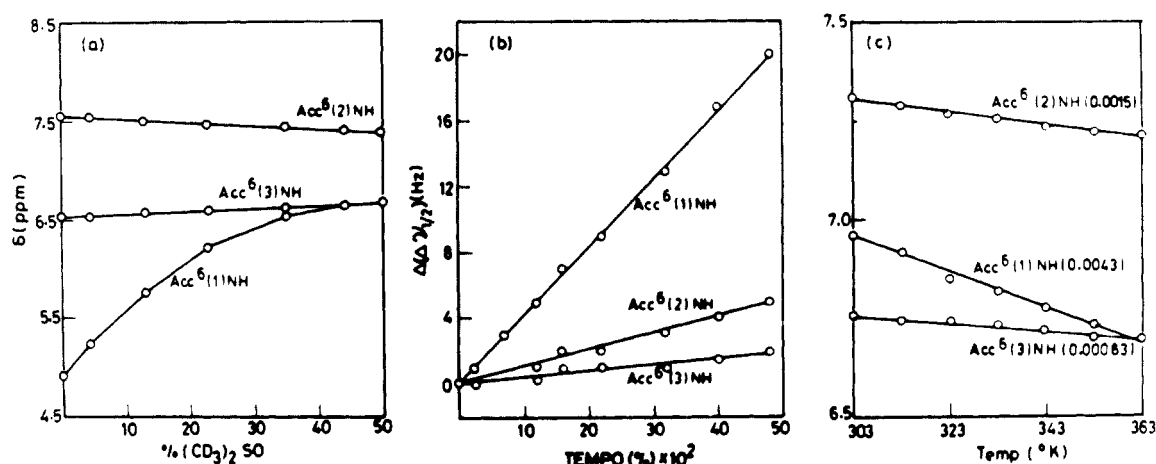


**Figure 9.** (a) Solvent dependence of NH chemical shifts in Boc-(Acc<sup>6</sup>)<sub>3</sub>-OMe (6) in  $\text{CDCl}_3$ – $(\text{CD}_3)_2\text{SO}$  mixtures. (b) Effect of Tempo on the line width of NH resonances in 6 in  $\text{CDCl}_3$ .  $\Delta(\delta\nu_{1/2})$  is the line broadening. (c) Temperature dependence of NH chemical shifts in  $(\text{CD}_3)_2\text{SO}$  for 6. Temperature coefficients ( $d\delta/dT$ ) are indicated in parentheses. Peptide concentration in all experiments is  $\sim 0.025$  M.

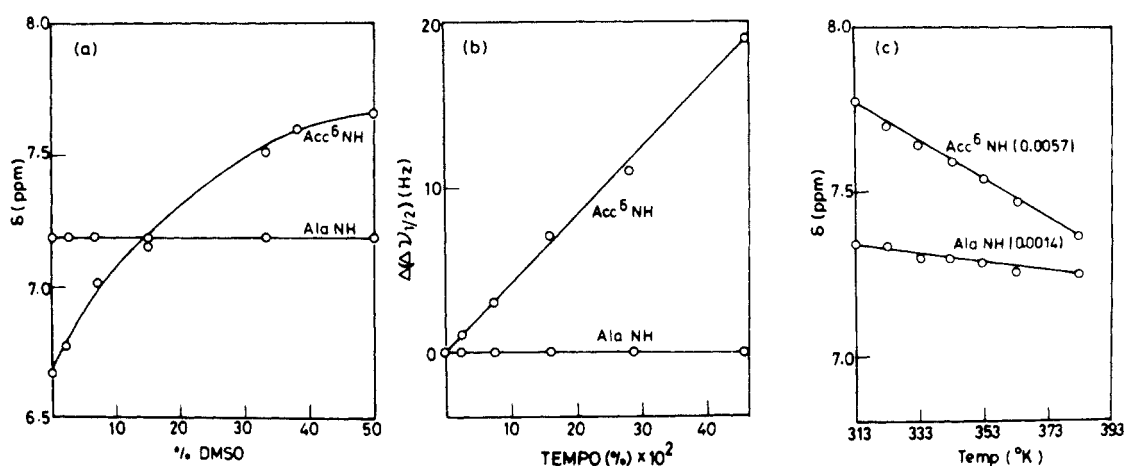


**Figure 10.** (a) Solvent dependence of NH chemical shifts in Boc-Pro-Acc<sup>6</sup>-Ala-OMe (7) in  $\text{CDCl}_3$ – $(\text{CD}_3)_2\text{SO}$  mixtures. (b) Effect of Tempo on the line width of NH resonance in 7 in  $\text{CDCl}_3$ .  $\Delta(\delta\nu_{1/2})$  is the line broadening. (c) Temperature dependence of NH chemical shifts in  $(\text{CD}_3)_2\text{SO}$  for 7.  $d\delta/dT$  values are indicated in parentheses. Peptides concentrations in all experiments is  $\sim 0.025$  M.

Table IV. The hydrogen bond parameters are given in Table V. The bond lengths and bond angles are largely unexceptional.

Peptide 6 adopts an almost ideal type III (III')  $\beta$ -turn conformation<sup>18,19</sup> with Acc<sup>6</sup>(1) ( $\phi = \pm 60.8^\circ$ ,  $\psi = \pm 29.5^\circ$ ) and Acc<sup>6</sup>(2) ( $\phi = \pm 60.5^\circ$ ,  $\psi = \pm 24.9^\circ$ ) as the  $i + 1$  and  $i + 2$  residues, respectively. The 4 $\rightarrow$ 1 intramolecular hydrogen bond (Boc CO $\cdots$ Acc<sup>6</sup>(3)NH) has an N $\cdots$ O distance of 3.076 Å which is in the range expected for intramolecular hydrogen bonds in peptides.<sup>20</sup> The third Acc<sup>6</sup> residue also adopts a conformation in the helical region but has a handedness opposite to that of the preceding residue. This feature has been consistently observed in crystal structures of Aib containing oligopeptides.<sup>3a</sup> The mean endocyclic torsion angles for the cyclohexane rings of the three Acc<sup>6</sup> residues are Acc<sup>6</sup>(1) 55.6 (8)°, Acc<sup>6</sup>(2) 55.4 (8)°, and Acc<sup>6</sup>(3) 54.0 (7)°. These values are very close to the expected torsion angles of 54.7° in cyclohexane, with a C–C–C bond angle of 111.5°.<sup>15</sup> A single intermolecular hydrogen bond between the Acc<sup>6</sup>(1) NH group and Acc<sup>6</sup>(2) CO groups of symmetry related molecules (N $\cdots$ O,

2.890 (5) Å) is observed in the crystal structure (Table V, Figure 7).

Peptide 7 adopts a type II  $\beta$ -turn conformation with Pro ( $\phi = -60.1^\circ$ ,  $\psi = 136.6^\circ$ ) and Acc<sup>6</sup> ( $\phi = 61.5^\circ$ ,  $\psi = 29.1^\circ$ ) as the  $i + 1$  and  $i + 2$  residues. A single intramolecular hydrogen bond is observed between the Boc CO and Ala NH groups (Figure 6). The N $\cdots$ O distance of 3.21 Å is at the upper limit of the range of values reported in a large number of peptide structures.<sup>20</sup> The  $\phi$ ,  $\psi$  values for Acc<sup>6</sup> deviate by  $\sim 20$ – $30^\circ$  from those expected in an ideal type II  $\beta$ -turn and result in a lengthening of the N $\cdots$ O distance. The Acc<sup>6</sup> residue again adopts a conformation in the left-handed  $3_{10}/\alpha$ -helical region of the  $\phi$ ,  $\psi$  map. The cyclohexane ring in 7 has a mean endocyclic torsion angle of 53.7 (4)°, which is representative of an almost ideal chair conformation. The pyrrolidine ring of Pro adopts two distinct conformations, with different occupancies. These are the C<sub>exo</sub><sup>γ</sup> (C(8)) and C<sub>endo</sub><sup>γ</sup> (C(80)) conformations, the ring having an approximate C<sub>s</sub> (envelope) symmetry.<sup>21</sup> A single intermolecular hydrogen bond between the Acc<sup>6</sup> NH and Acc<sup>6</sup> CO groups of symmetry related molecules (N $\cdots$ O, 2.90 Å) stabilizes the crystal structure (Table V, Figure 8).

All four Acc<sup>6</sup> residues observed in the crystal structures of peptides 6 and 7 adopt backbone conformations in the  $3_{10}/\alpha$ -helical regions of  $\phi$ ,  $\psi$  space. Thus all Acc<sup>6</sup> residue conformations determined by X-ray diffraction fall into these regions (Figure 2a)

(18) (a) Venkatachalam, C. M. *Biopolymers* **1968**, *6*, 1425–1436. (b) Rose, G. D.; Gierasch, L. M.; Smith, J. A. *Adv. Protein Chem.* **1985**, *37*, 1–109.

(19) The conformational angles in ideal  $\beta$ -turns are as follows: type I,  $\phi_{i+1} = -60^\circ$ ,  $\psi_{i+1} = -30^\circ$ ,  $\phi_{i+2} = -90^\circ$ ,  $\psi_{i+2} = 0^\circ$ ; type II,  $\phi_{i+1} = -60^\circ$ ,  $\psi_{i+1} = 120^\circ$ ,  $\phi_{i+2} = 80^\circ$ ,  $\psi_{i+2} = 0^\circ$ ; type III,  $\phi_{i+1} = -60^\circ$ ,  $\psi_{i+1} = -30^\circ$ ,  $\phi_{i+2} = -60^\circ$ ,  $\psi_{i+2} = -30^\circ$ . The enantiomeric type I', II', and III'  $\beta$ -turns are obtained by inverting the signs of all the torsion angles.

(20) (a) Karle, I. L. *The Peptides*; Gross, E., Meienhofer, J., Eds.; Academic Press: New York, 1981; Volume IV, pp 1–53. (b) Taylor, R.; Kennard, O.; Versichel, W. *Acta Crystallogr.* **1984**, *B40*, 280–288.

(21) (a) Ramachandran, G. N.; Lakshminarayanan, A. V.; Balasubramanian, R.; Tegoni, G. *Biochim. Biophys. Acta* **1970**, *221*, 165–181. (b) Ashida, T.; Kakudo, M. *Bull. Chem. Soc. Jpn.* **1974**, *47*, 1129–1133.

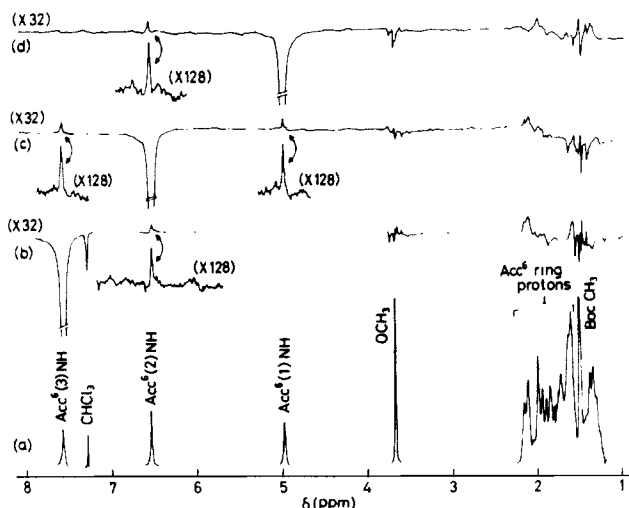


**Figure 11.** (a) 270-MHz  $^1\text{H}$  NMR spectrum of Boc-(Acc<sup>6</sup>)<sub>3</sub>-OMe (6) in  $\text{CDCl}_3$ . (b-d) Difference NOE spectra obtained by irradiation of NH resonances: (b) Acc<sup>6</sup>(3) NH, (c) Acc<sup>6</sup>(2) NH, (d) Acc<sup>6</sup>(1) NH. Vertical scale expansions are indicated against the traces. The difference spectra were recorded as described earlier,<sup>14</sup> using 1024 accumulations for both on and off resonance experiments, in each case. Peptide concentration  $\sim 0.05$  M.

providing overwhelming support for the theoretical predictions. The results also experimentally establish that Acc<sup>6</sup> residues can occur at either position ( $i + 1$ ,  $i + 2$ ) of type III  $\beta$ -turns or at the  $i + 2$  position of type II  $\beta$ -turns. These observations are relevant when employing Acc<sup>6</sup> residues to generate folded oligopeptide models.

**NMR Studies.**  $^1\text{H}$  NMR studies were carried out in order to determine whether the folded structures, determined for 6 and 7 in the solid state, are maintained in solution. The delineation of solvent inaccessible or intramolecularly hydrogen bonded NH groups was carried out with use of temperature and solvent dependence of NH chemical shifts and free radical induced line broadening of NH resonances.<sup>22</sup> The results of these experiments are summarized in Figures 9 and 10 for peptides 6 and 7, respectively. The assignments of NH resonances are trivial in 7. In 6, the upfield NH resonance in  $\text{CDCl}_3$  is assigned to the Acc<sup>6</sup>(1) NH (urethane) in  $\text{CDCl}_3$ .<sup>13</sup> The Acc<sup>6</sup>(2) NH and Acc<sup>6</sup>(3) NH resonances can be unambiguously identified by NOE experiments as described later. In peptide 6 the Acc<sup>6</sup>(2) and Acc<sup>6</sup>(3) NH groups display behavior characteristic of solvent shielded protons (relative insensitivity of chemical shifts to solvent composition in  $\text{CDCl}_3$ - $(\text{CD}_3)_2\text{SO}$  mixtures, insensitivity of line widths to the presence of the free radical 2,2,6,6-tetramethylpiperidine-1-oxyl (Tempo), and low  $d\delta/dT$  values ( $<0.003$  ppm/K) in  $(\text{CD}_3)_2\text{SO}$ .<sup>22</sup> The Acc<sup>6</sup>(1) NH is clearly solvent exposed (Figure 9). These results are consistent with a  $\beta$ -turn conformations for 6, in which Acc<sup>6</sup>(3) NH is involved in an intramolecular  $4 \rightarrow 1$  hydrogen bond with the Boc CO group, while Acc<sup>6</sup>(2) NH is sterically shielded from the solvent by the flanking cyclohexyl groups. Nuclear Overhauser effect (NOE) studies<sup>14,23</sup> illustrated in Figure 11 and summarized in Table VI permit determination of the nature of the  $\beta$ -turn<sup>14</sup> and assignment of the NH resonances to specific Acc<sup>6</sup> residues. Irradiation of the Acc<sup>6</sup>(1) NH results in an enhancement of  $\sim 1.9\%$  of the resonance at  $\delta$  6.53, which may then be assigned to the Acc<sup>6</sup>(2) NH group. There are no  $\beta$ -turn or other regular, sterically allowed conformations which bring the  $\text{N}_i\text{H}$  and  $\text{N}_{i+2}\text{H}$  protons to distances  $<3.0$  Å,<sup>24</sup> thus eliminating the possibility of

**Table VI.** Nuclear Overhauser Effect Data for Peptides 6 and 7

resonance		NOE (%)	H...H distance <sup>a</sup> (Å)
irradiated	obsd		
Boc-(Acc <sup>6</sup> ) <sub>3</sub> -OMe (6)			
Acc <sup>3</sup> (1) NH	Acc <sup>6</sup> (2) NH	1.9	2.637
	Acc <sup>6</sup> (3) NH		4.468
Acc <sup>6</sup> (2) NH	Acc <sup>6</sup> (1) NH	1.8	2.637
	Acc <sup>6</sup> (3) NH	2.5	2.804
Acc <sup>6</sup> (3) NH	Acc <sup>6</sup> (2) NH	1.2	2.804
	Acc <sup>6</sup> (1) NH		4.468
Boc-Pro-Acc <sup>6</sup> -Ala-OMe (7)			
Acc <sup>6</sup> NH	Pro C <sup>α</sup> H	8.5	2.051
Pro C <sup>α</sup> H	Acc <sup>6</sup> NH	3.4	2.051

<sup>a</sup> H---H distances are calculated from the hydrogen coordinates in the crystal structures.

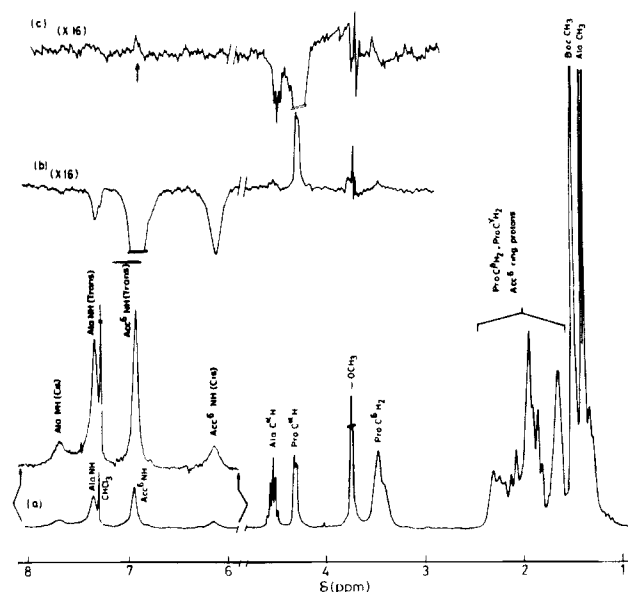


**Figure 12.** (a) 270-MHz  $^1\text{H}$  NMR spectrum of Boc-Pro-Acc<sup>6</sup>-Ala-OMe (7) in  $\text{CDCl}_3$ . Note the presence of lines due to *cis* Boc-Pro conformers. (b and c) Difference NOE spectra obtained by irradiation of (b) Acc<sup>6</sup> NH and (c) Pro C $\alpha$ H resonances. In spectrum b note the transfer of saturation to minor *cis* conformer resonance. In spectrum c the position of the observed NOE is indicated by an arrow. Vertical scale expansions are indicated. In the NOE experiments 128 accumulations were used. Peptide concentration  $\sim 0.05$  M.

an NOE between Acc<sup>6</sup>(1) NH and Acc<sup>6</sup>(3) NH protons. Irradiation of the Acc<sup>6</sup>(2) NH resonance results in small enhancements of the Acc<sup>6</sup>(1) and Acc<sup>6</sup>(3) NH resonances (Figure 11, Table VI). The observation of successive  $\text{N}_i\text{H} \cdots \text{N}_{i+1}\text{H}$  NOEs is expected in  $3_{10}/\alpha$ -helical conformations,<sup>24,25</sup> with  $\phi_i \sim \phi_{i+1} \sim \pm 50^\circ \pm 20^\circ$  and  $\psi_i \sim \psi_{i+1} \sim 40^\circ \pm 20^\circ$ . This is consistent with a type III  $\beta$ -turn conformation<sup>19</sup> in 6, similar to that observed in the solid state. The NH---NH distances determined in the crystal structure (Table VI) are compatible with the NOE data. The magnitudes of the observed NOEs are very small. This is likely to be the case because of alternative relaxation pathways available for NH protons. The estimated NOEs are likely to be subject to considerable error. Nevertheless, in conjunction with hydrogen bonding studies, they provide qualitative support for the retention of the solid-state conformation of 6, in solution also.

In Boc-Pro-Acc<sup>6</sup>-Ala-OMe (7) the NMR data summarized in Figure 10 clearly establish that the Ala NH group is strongly solvent shielded, while the Acc<sup>6</sup> NH is fully exposed to solvent. The data then support the involvement of Ala NH in an intra-

(22) (a) Wüthrich, K. *NMR in Biological Research: Peptides and Proteins*; North-Holland: Amsterdam, 1976. (b) Kessler, H. *Angew. Chem., Int. Ed. Engl.* **1982**, *21*, 512-523. (c) Hruby, V. J. *Chemistry and Biochemistry of Amino Acids, Peptides and Proteins*; Weinstein, B., Ed.; Marcel Dekker: New York, 1974; Vol. 3, pp 1-188.

(23) Bothner-By, A. A. *Magnetic Resonance in Biology*; Shulman, R. G., Ed.; Academic Press: New York, 1979; pp 177-219.

(24) Billeter, M.; Braun, W.; Wüthrich, K. *J. Mol. Biol.* **1982**, *155*, 321-346.

(25) Shenderovich, M. D.; Nikiforovich, G. V.; Chipens, G. I. *J. Magn. Reson.* **1984**, *59*, 1-12.

(26) (a) De Tar, D. F.; Luthra, N. *J. Am. Chem. Soc.* **1977**, *99*, 1232-1244. (b) Gratwohl, C.; Wüthrich, K. *Biopolymers* **1976**, *15*, 2025-2041.

molecular hydrogen bond, presumably of the 4→1 type, stabilizing a  $\beta$ -turn conformation. NOE studies in  $\text{CDCl}_3$  solution serve to establish the nature of the  $\beta$ -turn. Irradiation of the  $\text{Acc}^6$  NH resonance results in an NOE of 8.5% on the Pro  $\text{C}^\alpha\text{H}$  proton (Figure 12, Table VI), in agreement with a type II  $\beta$ -turn conformation having Pro and  $\text{Acc}^6$  at the  $i + 1$  and  $i + 2$  positions. In the reverse experiment, irradiation of the Pro  $\text{C}^\alpha\text{H}$  resonance results in a much smaller NOE of 3–4% on the  $\text{Acc}^6$  NH proton (Figure 12), suggesting that alternative relaxation pathways are available to the  $\text{Acc}^6$  NH proton. Indeed, for an axial orientation of the amino group in  $\text{Acc}^6$ , the distances between the NH proton and the axial protons at the two  $\text{C}^\gamma$  atoms are very short, in most sterically allowed conformations. This should result in appreciable contributions to dipolar relaxation of the NH proton. In the crystal structure of **7**, the observed distances are  $\text{N}(2)\text{H} \cdots \text{C}(13)\text{H}_{\text{ax}} = 2.99 \text{ \AA}$  and  $\text{N}(2)\text{H} \cdots \text{C}(15)\text{H}_{\text{ax}} = 2.314 \text{ \AA}$ . The  $\text{Acc}^6$  NH( $\text{N}(2)\text{H} \cdots \text{Pro C}^\alpha\text{H}(\text{C}(6)\text{H})$ ) distance in the crystal is 2.05  $\text{ \AA}$ , compatible with the large NOE observed on the Pro  $\text{C}^\alpha\text{H}$  proton, when the  $\text{Acc}^6$  NH resonance is irradiated. A notable feature of the NMR spectrum in Figure 12 is the observation of additional resonances in the NH region, assignable to a cis conformation (25%)<sup>27</sup> about the Boc-Pro bond. Appreciable transfer of saturation to the minor resonance at  $\delta$  6.11 is seen on irradiating the major  $\text{Acc}^6$  NH peak at  $\delta$  6.92 (Figure 12b), confirming the assignment of the minor resonance, to a conformation which is in slow exchange with the major species. For cis conformations of the Boc-Pro bond the intramolecular 4→1 hydrogen bond will be broken. The data suggest that the conformation observed in the crystal structure corresponds to the major conformer in  $\text{CDCl}_3$  solutions of **7**.

Peptides **6** and **7** thus appear to maintain well-defined, folded backbone conformations in solution, similar to those observed in the solid state.

#### Implications for Conformational Design

The theoretical and experimental results described above establish that  $\text{Acc}^6$  residues impart considerable stereochemical rigidity to peptide backbones and are constrained to adopt conformations in the  $3_{10}/\alpha$ -helical regions of  $\phi, \psi$  space.  $\text{Acc}^6$  residues can be accommodated in either position of type III (III')  $\beta$ -turns or at the  $i + 2$  position of type II (II')  $\beta$ -turns. Considerable recent interest has been focussed on the development of conformationally constrained analogues of biologically active peptides.<sup>27</sup> The availability of highly active, structurally rigid agonists is of value in delineating the nature of receptor bound conformations. Recent studies in this area are exemplified by the development of active cyclic analogues of somatostatin,<sup>28</sup>  $\alpha$ -melanocyte stimulating

hormone,<sup>30</sup> and renin inhibitors.<sup>31</sup>  $\alpha, \alpha$ -Dialkylated residues are of particular importance in developing conformationally rigid acyclic analogues.<sup>27</sup> Aib containing analogues of enkephalins<sup>32</sup> and chemotactic peptides<sup>33</sup> have been studied. In these studies Gly and Leu residues have been replaced by Aib. Relatively few reports on the use of 1-aminocycloalkancarboxylic acids ( $\text{Acc}^n$ ) have appeared,<sup>34</sup> but recent studies on chemotactic peptides<sup>7</sup> and aspartame analogues<sup>35</sup> suggest that the greater bulk of the  $\text{Acc}^n$  side chain ( $n \geq 5$ ) may be of value in binding to hydrophobic pockets at the receptor site. Systematic variations<sup>35</sup> in the size of the  $\text{Acc}^n$  group can permit an estimation of the size of the binding site for this residue. The backbone conformational restrictions imposed by  $\text{Acc}^6$  residues and the similarity of the side chain bulk to that of Val, Leu, and Ile groups suggests that  $\text{Acc}^6$  residues should be an important component in the armamentarium of the peptide chemist, in designing stereochemically rigid analogues of biologically active peptides. A comparison of the results obtained in this study for  $\text{Acc}^6$ , together with earlier reports on  $\alpha, \alpha$ -dialkylated residues,<sup>4</sup> clearly establishes that this class of amino acids can be used to stabilize folded, helical structures or fully extended chains, depending on whether cyclic or acyclic substituents are employed.

**Acknowledgment.** The assistance of S. Raghothama in the NOE experiments is gratefully acknowledged. This research was partially supported by a grant from the Department of Atomic Energy, Government of India.

**Registry No.** **6**, 103732-16-7; **7**, 103732-17-8; Ac- $\text{Acc}^6$ -NHMe, 103732-15-6; Ac-Aib-NHMe, 42037-26-3; Ac-Dpg-NHMe, 93039-01-1.

**Supplementary Material Available:** Tables (S-1–S4, S7, and S8) of bond lengths, bond angles used in obtaining average geometry, anisotropic temperature factors and hydrogen coordinates, and bond lengths and bond angles for crystal structures of Boc-( $\text{Acc}^6$ )<sub>3</sub>-OMe (**6**) and Boc-Pro- $\text{Acc}^6$ -Ala-OMe (**7**) (9 pages); tables (S5 and S6) of calculated and observed structure factors for **6** and **7** (22 pages). Ordering information is given on any current masthead page.

(27) (a) Spatola, A. F. *Chemistry and Biochemistry of Amino Acids, Peptides and Proteins*; Weinstein, B., Ed.; Marcel Dekker: New York, 1983; Vol. VII, pp 267–357. (b) Hruby, V. J. *Life Sci.* **1982**, *31*, 189–199.

(28) Veber, D. F.; Freidinger, R. M.; Schwenk-Perlow, D.; Paleveda, W. J., Jr.; Holly, F. W.; Strachan, R. G.; Nutt, R. F.; Arison, B. H.; Homnick, C.; Randall, W. C.; Glitzer, M. S.; Saperstein, R.; Hirschmann, R. *Nature (London)* **1981**, *292*, 55–58.

(29) Schiller, P. W. *The Peptides: Analysis, Synthesis, Biology*; Udenfriend, S., Meienhofer, J., Eds.; Academic Press: New York, 1985; Vol. 7, pp 219–269.

(30) Hadley, M. E.; Anderson, B.; Heward, C. B.; Sawyer, T. K.; Hruby, V. J. *Science* **1981**, *213*, 1025–1027.

(31) Boger, J. *Peptides. Structure and Function*; Hruby, V. J., Rich, D. H., Eds.; Peirce Chemical Co.: Rockford, IL, 1983; pp 569–578.

(32) Sudha, T. S.; Balaram, P. *Int. J. Pept. Protein Res.* **1983**, *21*, 381–388.

(33) Iqbal, M.; Balaram, P.; Showell, H. J.; Freer, R. J.; Becker, E. L. *FEBS Lett.* **1984**, *165*, 171–174.

(34) (a) Tailleux, P.; Berlinguet, L. *Can. J. Chem.* **1962**, *40*, 2214–2217.

(b) Park, W. K.; Choi, C.; Rioux, F.; Regoli, D. *Can. J. Chem.* **1974**, *52*, 113–119. (c) Jorgenson, E. C.; Rapaka, S. R.; Windridge, G. C.; Lee, T. C. *J. Med. Chem.* **1971**, *14*, 904–906.

(35) (a) Tsang, J. W.; Schmied, B.; Nyfeler, R.; Goodman, M. *J. Med. Chem.* **1984**, *27*, 1663–1668. (b) Rodriguez, M.; Bland, J. M.; Tsang, J. W.; Goodman, M. *J. Med. Chem.* **1985**, *28*, 1527–1529. (c) Goodman, M. *Biopolymers* **1985**, *24*, 137–155.